17th Australasian Wind Engineering Society Workshop
Wellington, New Zealand
12-13 February 2015

Numerical investigation of distributed trailing edge suction for wind turbine aerofoils using CFD

V.V. Dighe[1], **J.E. Cater**[2]

[1]Research Student, Department of Engineering Science
University of Auckland, Auckland 1142, New Zealand

[2]Senior Lecturer, Department of Engineering Science
University of Auckland, Auckland 1142, New Zealand

Abstract

The study investigates the effect of distributed suction on the dynamics of flow over the boundary layer of a wind turbine aerofoil with a NACA 63-415 profile. Steady state, two-dimensional CFD calculations were performed for two different aerofoil configurations at a Reynolds number of 4×10^6. The Navier-Stokes solver, ANSYS Fluent® was used to perform simulations and the results were obtained using the two-equation k-ω SST turbulence model. The solutions were computed for angles of attack ranging from 2-16 degrees to estimate aerodynamic characteristics in terms of lift and drag coefficients. The results of this study show that distributed trailing edge suction has a positive effect on the performance characteristics and on the downstream wake profile.

Introduction

The wind energy industry has been expanding rapidly with 35 GW of wind power capacity added in 2013, for a total of 318 GW (Martinot, 2014). The year witnessed 85 countries participating in commercial wind activity, and almost 24 countries reported more than 1 GW capacity by the year-end. The impetus was awareness of fossil fuel based electricity production, which has been depleting rapidly over the past few decades. The majority of installations were seen in the Non-OECD countries with China leading the market (Ahmed and Cameron, 2014). The European Union has a cumulative total of 37% of the worlds total wind energy capacity and Asia has a total of 36%.

The need to design larger and more efficient wind turbines has become the principal focus in wind turbine research (Ackermann, 2005). Wind turbine design is a process of identifying and implementing a structure capable of extracting maximum energy from the wind. Betz in 1919 showed that for an ideal wind extraction device, the laws of mass and energy conservation allowed extraction of no more than 59.3% of energy from the wind (Burton et al., 2011). As demand of energy increases, turbine designs continue to evolve as manufacturers are trying to mitigate the costs and increase the yield.

Flow control theory remains one of the complex discussions in wind turbine applications and numerous concepts are currently being investigated around the world (Zayas et al., 2006). The Microtab and Gurney Flap can be used as a performance enhancement or a load mitigation device, but it may result in structural and fatigue loading as the size of the wind turbine blade increases. Scot presented various concepts for the active control techniques for wind turbine application (Johnson et al., 2008). The study performed by Chanin found that leading edge blowing from the blade surface leads to increased torque and power production (Tongchitpakdee et al., 2006).

The main purpose of the present study is to improve the aerodynamic characteristics of a wind turbine aerofoil using distributed trailing edge suction. Numerical simulations for different suction velocities were performed in the study.

Numerical Method

The numerical study consisted of NACA 63-415 aerofoil, in its original form and after the implementation of flow control. The experimental results used for the validation consists of tests performed at the VELUX wind tunnel facility designed at Risø National Laboratory, Denmark (Bak, 2000).

The geometry and mesh topology for both the aerofoil configurations consist of a C-grid mesh, with a wall spacing of 1×10^{-4} m. The grid spacing ($y^+ < 5$) is sufficient to resolve the transition region and the viscous sub-layer (Manual, 2012). The computational domain was extended to 6 chord lengths at the inlet and 12 chord lengths at the outlet. The distributed suction extended from x/c = 50% to 95% of the aerofoil chord length (1m).

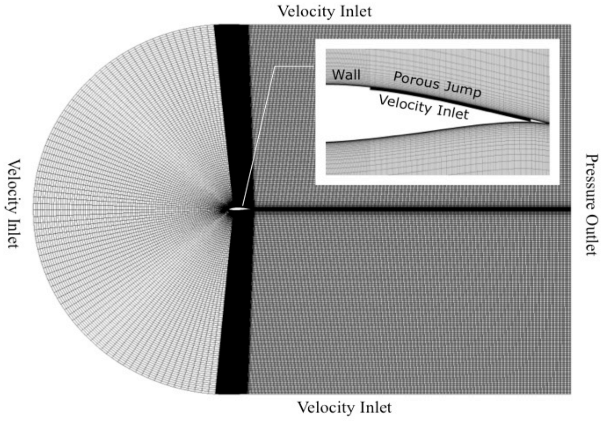

Figure 1. This figure shows a structured mesh around the modified aerofoil with boundary conditions explained.

Turbulence model validation was performed by computationally analysing the original aerofoil and comparing the lift, drag and pressure coefficients with the experimental data. Based on the validation study, the k-ω SST turbulence model was chosen for all computations as it proved able to resolve boundary layer flows, adverse pressure gradients and separated flows.

The domain inlet uses a developed turbulent velocity along with all relevant scalar properties of the flow. The flow is initialised at the velocity inlet BC (boundary condition) for a freestream Reynolds number of 4×10^6. At the domain outlet, a constant average pressure condition is set to zero and defined by pressure outlet BC. The aerofoil surface is represented using no-slip wall that sets up the surface roughness effect. Figure 1 shows the modified aerofoil in detail. The modification consists of replacing a part of the wall BC with a porous region. At the upper surface, porous jump BC allowed the flow to escape the surface and was regulated by velocity inlet at the bottom. The sides of the modified surface were defined by no-slip shear surfaces.

The final grid for the original and the modified aerofoil consisted of 129,710 and 313,998 structured cells respectively. The simulations were performed on a desktop system with an Intel® Core™ i5 quad core processor with 12 GB of RAM.

Data Acquisition and Analysis

The approach used for 2D steady-state simulations produces a large amount of data. For carrying out the aerodynamic performance analysis for the two different aerofoil configurations, *lift* and *drag* coefficient calculation is enabled through the monitor panel available in Fluent. The coefficient uses the reference values to initialize the flow, which updates at each iteration. The residuals converged rapidly falling below the convergence criterion of 10^{-6} in 100 iterations for the simple case, and 300 iterations for the modified case.

The governing equations for the flow through the porous media is described with pressure drop that is a function of the seepage velocity through the porous media (Nield and Bejan, 2006). Fluent does not update force coefficient values for the porous region, which needs to be evaluated separately. An analytical approach to define the same is developed using the *Custom Field Function* available in Fluent. It allows the generation of custom field functions based on the existing functions, using calculator operators.

The *lift* and *drag* evaluation for the porous medium requires the consideration of the pressure and viscous terms in the calculations. The pressure lift, L_P and pressure drag, D_P is defined by:

$$L_P = \int pn.k dA_y \tag{1}$$

$$D_P = \int pn.i dA_x \tag{2}$$

where p is the static pressure, dA_X and dA_Y are the x-face area and y-face area obtained from Fluent. n, i and k are the direction vectors, which are based on the angle of attack.

The determination of the viscous force D_V on the porous media would require consideration of various parameters for its approximation. Nield referred this phenomenon as *Quadratic Drag,* where Forcheimer's equation is used to model flow through the porous media in terms of seepage velocity (Nield and Bejan, 2006). Using the same approach and replacing the seepage velocity by suction velocity, the function derived is,

$$\Delta p = \left(\frac{\mu}{\alpha}\hat{u} + \frac{1}{2}C\rho|\hat{u}|\hat{u}\right)\Delta x = \frac{D_V}{A} \tag{3}$$

where Δp is the pressure drop across the porous surface, α is the permeability and C is the pressure jump coefficient calculated using inertial loss factor across the porous boundary. $\hat{u}$ is the suction velocity, which is normal to the surface and Δx is the porous media thickness. The distance through the porous media Δx depends on the angle of attack and is given by,

$$\Delta x = \frac{\Delta x_{90}}{\sin(\theta)} \tag{4}$$

A series of simulations for the modified aerofoil at different angles of attack have been performed. The depth of the porous medium was 0.001 m, and tests carried for five different suction velocities: 0.25, 0.5, 0.75, 1 and 2 m/s. The overall *lift* and *drag* coefficients were found for the modified aerofoil and compared against the original aerofoil.

Results

A comparison of computational C_l and C_d with the experimental data at various angles of attack is shown in Figure 2(a) and 2(b). It is observed that the C_l and C_d for the simple aerofoil configuration is in good agreement with the experimental values until the stall angle, α = 12°. The k-ω SST turbulence model underpredicts C_l by ≈ 9.5% and overpredicts C_d by ≈ 15% for angles beyond stall.

It can also be observed from Figure 2(a) and 2(b) that suction has a positive effect on the C_l and C_d values for small suction velocity; C_d increases beyond a suction velocity of 1 m/s and deteriorates the overall aerodynamic performance shown in Figure 2(c). The maximum *lift/drag* ratio is achieved at the suction velocity of 0.5 m/s. Also, the original optimum angle of attack, α = 4° has now changed to α = 6° with suction.

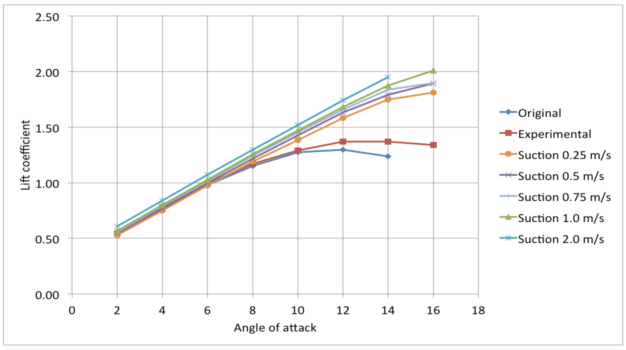

(a) C_l vs. α

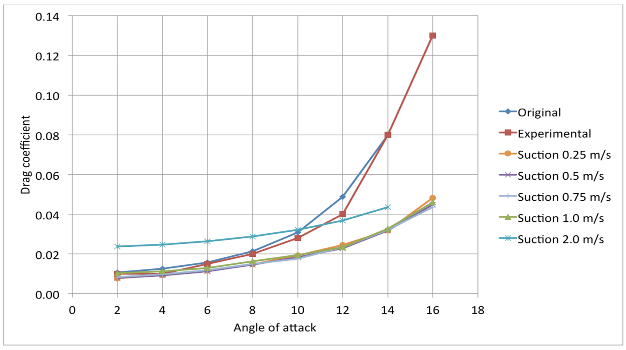

(b) C_d vs. α

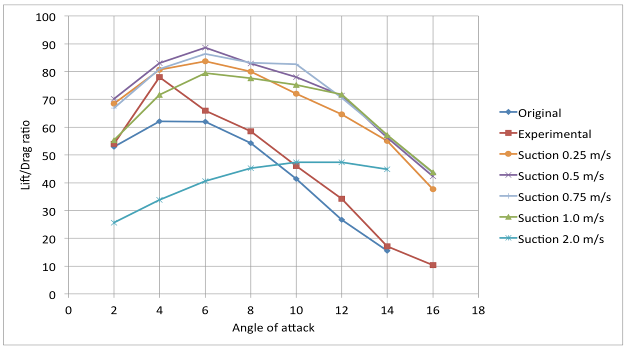

(c) L/D vs. α

Figure 2. Comparison plots for the aerodynamic characteristics of the original aerofoil with the suction cases for a Re = 4×10^6.

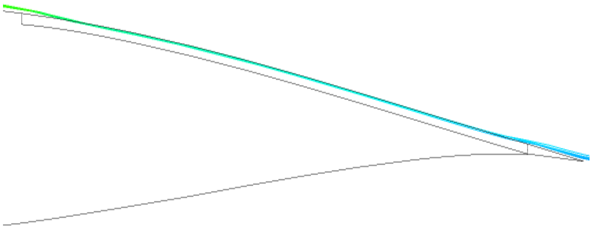

(a) Suction velocity = 0.25 m/s

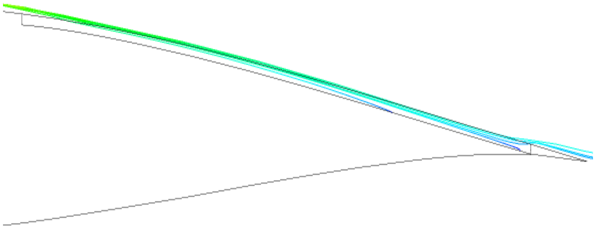

(b) Suction velocity = 0.5 m/s

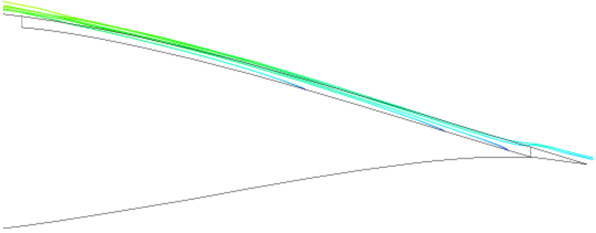

(c) Suction velocity = 0.75 m/s

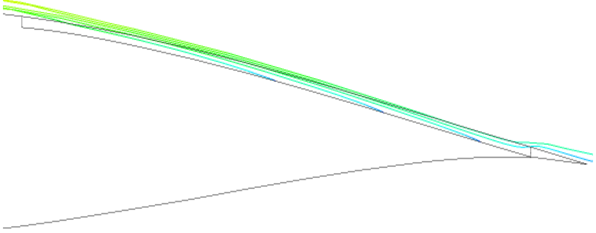

(d) Suction velocity = 1.0 m/s

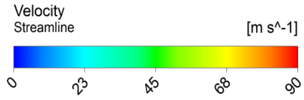

Figure 3. Velocity streamlines around the trailing edge of the modified aerofoil for different suction velocities at α = 6°

Most of the aerodynamic losses are a consequence of the creation of a boundary layer on the wind turbine blade surface (Hodson, 1984). Figure 3 shows the streamlines along the aerofoil trailing edge at α = 6° with different suction velocities. When the suction velocity is set to 0.25 m/s as in Figure 3(a), the flow escaping the porous region is relatively small. In contrast, for higher suction velocities, Figure 3(b), (c) and (d), the low momentum layers from the bottom of the boundary layer are pulled into the porous slots. This would allow the higher energy air from the outer layers to move closer to the surface, which gives the boundary layer a fuller velocity profile.

Flow control by suction prevents early separation (indicated by delay in stall angle, (Figure 2a) as the boundary layer thickness decreases. The suction effect creates higher effective streamline from the air moving over the aerofoil surface and as a consequence, the pressure drag decreases. Combining these advantages, the lift-drag ratio for α = 6° increases significantly.

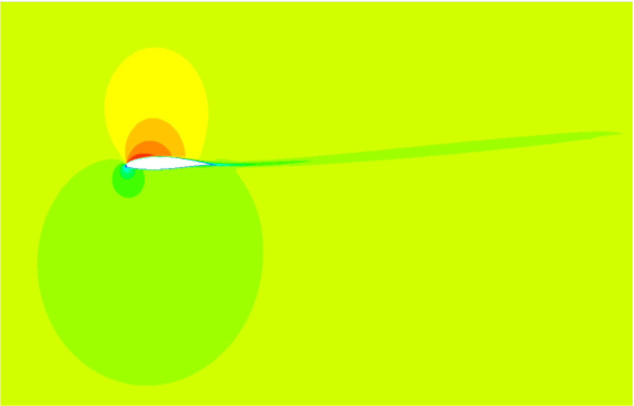

(a) Wake profile of the original aerofoil at α = 6°

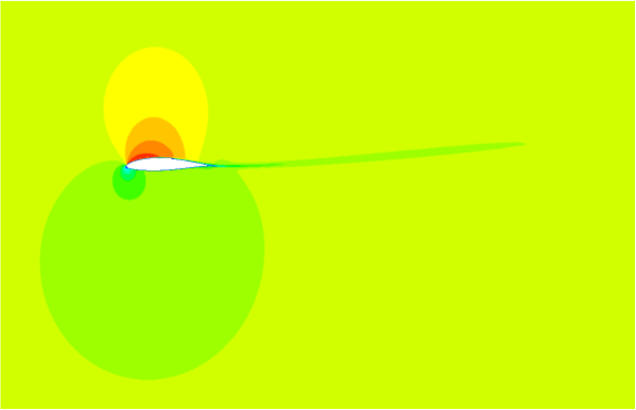

(b) Wake profile of the aerofoil with suction velocity of 0.5 m/s at α = 6°

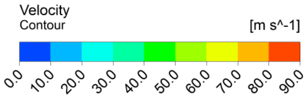

Figure 4. Velocity contours to illustrate the wake momentum loss for different aerofoil configuration. (a) No suction (b) Suction = 0.5 m/s

In Figure 4, velocity field associated with the downstream wake is shown for the suction and the non-suction case, for α = 6°. Studies by Nakayama suggested that the downstream wake has the largest deficit in momentum and width (Nakayama et al., 1990). The velocity field shown in Figure 4 shows a shift in the stream-wise flow, which is indicated by a broader wake in Figure 4(a).

The improvement in the wake profile as seen in Figure 4(b) is a result of a change in the stream-wise momentum flux, which is a measure of profile drag. An aerofoil at a moderate angle of attack has a minimum-pressure point at the leading edge. The pressure aft of this point is subjected to an adverse gradient, and this results in transition from a laminar flow to a turbulent flow. Suction application favours the existence of laminar boundary layer over a larger area, and reduces the width of the downstream wake profile. A more stable boundary layer is maintained and the transition to turbulence is delayed.

Visualization of the surface flow by means of streamlines for α = 6° is shown in Figure 5. The application of suction, as Figure 5(b) shows, reduces the trailing edge boundary layer thickness, which is directly related to the trailing edge noise in the tip region for wind turbine applications (Brooks et al., 1989). The suction technique alters the trailing edge flow, keeping it attached to a greater extent than in the aerofoil without suction, Figure 5(a).

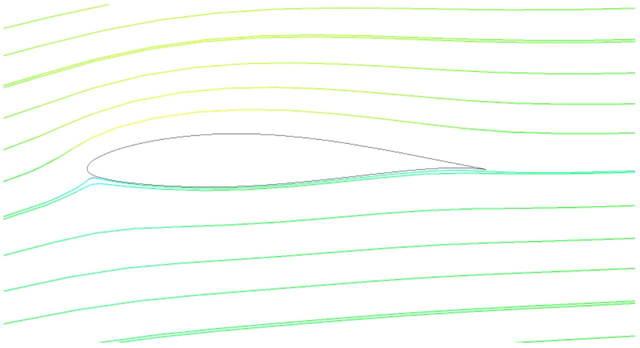

(a) No suction

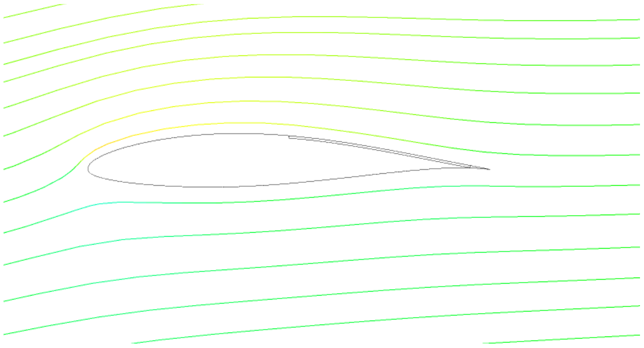

(b) Suction

Figure 5. Flow streamlines around the aerofoil surface at α = 6° for the suction and the non-suction case.

The amount of suction is the key factor to achieve improvement in the aerodynamic performance. Greater suction velocity would improve the lift characteristics, but would adversely affect the drag coefficient. Also, power is needed to obtain drag reduction. The optimum condition would be when the total drag (aerodynamic drag and suction power converted to equivalent drag) is smaller for the modified aerofoil than the original aerofoil.

Conclusions

In the study, flow control by suction is presented for the aerodynamic performance of the NACA 63-415 wind turbine aerofoil. The k-ω SST turbulence model was used after successful validation with the experimental data available. Computational simulations for five different suction velocities were performed and definite trends in C_l and C_d were observed, which were accompanied by an analytical study of porous flow modelling. Contour and streamline plots were studied to analyse the flow and the wake characteristics downstream of the aerofoil. Results from this study show that flow control by suction has the best performance when the suction velocity = 0.5 m/s for α = 6°. Also flow control implementation delays stall angle of the aerofoil by 4°, which previously stalled at α = 12° for Re = 4×10^6.

Although only an aerofoil application has been considered in the present study, the techniques of flow control by suction can be applied to the numerical study of full-scale turbine blade models at the cost of high computational resources. Boundary layer control by suction may address the problem of unsteady aerodynamic loads resulting from gusts and upwind wakes by maintaining an attached flow (Johansen, 2006). The integration of the suction technology into the blade element would increase the cost, but the increased torque and power output of the wind turbine may compensate.

Acknowledgments

This study was supervised by Dr. John Cater and was supported by the resources available at the Engineering Science department, University of Auckland. The author would also like to thank in particular Sahan Wasala, Associate Professor Donald Nield and Roland Broers for their timely inputs.

References

Ackermann T. (ed) (2005) Wind power in power systems (Vol. 140) Chichester, John Wiley.

Ahmed & Cameron M (2014) The challenges and possible solutions of horizontal axis wind turbines as a clean energy solution for the future. Renewable and Sustainable Energy Reviews, 38, 439-460.

Bak C, Fuglsang P, Johansen J, & Antoniou I (2000). Wind tunnel tests of the NACA 63-415 and a modified NACA 63-415 airfoil.

Brooks T F, Pope D S, & Marcolini M A (1989) Airfoil self-noise and prediction (Vol. 1218) National Aeronautics and Space Administration, Office of Management, Scientific and Technical Information Division.

Burton T, Sharpe D, & Jenkins N (2011) Handbook of wind energy.

Hodson H P (1984) Boundary layer and loss measurements on the rotor of an axial-flow turbine. Journal of Engineering for Gas Turbines and Power,106(2), 391-399.

Johansen J & Sørensen N N (2006). Aerodynamic investigation of winglets on wind turbine blades using CFD.

Johnson S J & Berg D E (2008). Active load control techniques for wind turbines.

Manual F (2012) Manual and user guide of Fluent Software, Fluent Inc.

Martinot E (2014) Renewables 2014 global status report, DIANE Publishing.

Nakayama A, Kreplin H P & Morgan H L (1990). Experimental investigation of flowfield about a multielement airfoil, AIAA Journal, 28(1), 14-21.

Nield D A & Bejan A (2006) Convection in porous media, Springer.

Tongchitpakdee C, Benjanirat S, & Sankar L N (2006) Numerical studies of the effects of active and passive circulation enhancement concepts on wind turbine performance, Journal of Solar Energy Engineering, 128(4), 432-444.

Zayas J R, Van D, Chow R, Baker J P & Mayda E A (2006) Active aerodynamic load control for wind turbine blades, European Wind Energy Conference, Athens, Greece.